

Using advanced discretization techniques to simulate the suturing process

Ana Guerra¹, Jorge Belinha², Renato Natal Jorge³

¹ aguerra@inegi.up.pt; INEGI, Rua Dr. Roberto Frias, 400, 4200-465; Porto; Portugal

² job@isep.ipp.pt; ISEP, Rua Dr. António Bernardino de Almeida, 431, 4249-015; Porto; Portugal

³ rnatal@fe.up.pt; FEUP, Rua Dr. Roberto Frias, 4200-465 Porto, Portugal

Abstract

Wounds or cuts in human skin are very common. Superficial wounds normally heal in short time; however, deep wounds usually required clinical intervention such as sutures to provide the wound closure and timely healing. This process affects the mechanical behaviour of the skin. Advanced discretization techniques, such as finite element method (FEM) and meshless methods can be used to predict the geometry of surgical incisions and to analyse stress and strain distribution in the skin aiming to improve scar formation. In this study we constructed 2D models to simulate the suturing process and to analyse the stress and strain fields obtained, using FEM and natural neighbour radial point interpolation method (NNRPIM) analysis. The simulations' results demonstrated that the highest levels of stress and strain were observed in the area around the wound, in both techniques used. Although this is a preliminary study to estimate the performance of numerical methods in the analysis of stress profile distribution in the human skin, it was possible to conclude that both FEM and NNRPIM are valid tools. Furthermore, the materials used in the simulations were well characterized in terms of elasticity. In the future works, it is intended to refine the model parameters and to include the hyperelastic and the anisotropic behaviour of the human skin.

DOI: 10.5281/zenodo.4669670

Article Info

Keywords

Finite element method
Natural Neighbour Radial
Point Interpolation Method
Human skin
Stress and strain fields

Article History

Received: 07/09/2020
Revised: 02/11/2020
Accepted: 25/01/2021

1 Introduction

Human skin is an important physical barrier between the body and the external environment being the first line of defence against any injury. This organ is composed by three layers. The epidermis (first layer) is very thin and its contribution to the mechanical behaviour of the skin is minimal. The dermis (second layer with approximately 2 mm of thickness) is responsible for the skin's mechanical properties and it provides structural and nutritional support to the skin. The hypodermis (third layer) is mainly composed by fat connective tissue that connects the dermis with the skeletal components. Each skin layer possesses its individual biological structure and its specific mechanical properties [1].

Skin wounds may be a result of traumatic accidents, surgery incisions, burns or due to long periods of immobilization. Superficial skin wounds normally heal in short time; however, deep wound usually required clinical intervention such as sutures to close and avoid blood lose and infection. The suturing process success is based in the surgeon's experience and there is no rigorous protocol to what is right or wrong technique [2]. Accordingly, the use of numerical simulation to analyse the mechanical behaviour of the skin aroused the interest of surgeons. Advanced discretization techniques, such as finite element method (FEM) and meshless methods can be used to predict the geometry of surgical incisions [3] and to analyse stress distribution in the skin [4] in order to reduce scar formation. Stress plays an important role in wound healing and in scar evolution. Accordingly, analyse stress theoretically is demanded, since no invasive or non-invasive technique to measure stress directly is available. This will be very useful in order to minimize negative outcomes such as permanent marks and high stress that reduces blood flow and facilitate the occurrence of hypertrophic scars [5].

In this work, we constructed 2D models simulating the suture process and we performed a linear elasto-static analysis of the stress and strain fields obtaining in each model, using both FEM and Natural Neighbour Radial Point Interpolation Method (NNRPIM). Moreover, the efficiency of both numerical methods used will be addressed.



2. Methods

2.1. Numerical analysis

FEM and NNRPIM are very useful to simulate biomechanical problems given its possibility to deal with complex geometries, loads and different material properties.

FEM is a mesh-dependent method, in which the domain is discretized with a finite number of interconnected elements forming a mesh. The first step in FEM is to obtain the discretized mesh and then the interpolation function can be reached. The polynomials functions are used to interpolate the field variables over the element. To obtain the discrete equation system, we used the Galerkin method. In order to achieve the global equation system, we need to combine the local element equations for all elements used for the discretization. Accordingly, the global equation system can be solved [6].

In meshless methods, such as NNRPIM, the domain is discretized with a free nodal distribution and the field functions are approximated within an influence-domain rather than an element [7]. In NNRPIM, since there is no predefined nodal interdependency, the nodal connectivity has to be enforced after the nodal discretization. Accordingly, the nodal connectivity is obtained using the natural neighbour concept with the partition of the discretized domain into a set of Voronoï cells. To each one of these cells is associated with only one node [8]. Then the background integration mesh should be constructed. For the numerical integration, NNRPIM uses the Galerkin weak form, being necessary to use a background integration mesh. The integration mesh is obtained using solely the nodal distribution, the previously constructed Voronoï diagram [9]. The Delaunay triangulation is used to subdivided the area of each Voronoï cell in several sub-areas. Finally, the discrete equation system, using the approximation or interpolations shape functions, can be achieved. In NNRPIM, the interpolation shape function combines a radial basis function with a polynomial basis function to obtain the approximation. The interpolation functions possess the Kronecker delta property, which means that the obtained function passes through all scattered points in the influence domain. Accordingly, this property simplify the imposition of the essential boundary conditions [7].

2.2. Solid mechanics

When solids are subjected to loads or forces they become stressed which results in strain, that can be interpreted as deformation or displacement [7]. Solid mechanics is focused in studding the relationship between stress and strain and the relationship between strain and displacements. In this work, only linear elastic materials are considered. It means that the relationship between stress and strain is assumed to be linear and the deformation in the solid caused by loading disappears fully with the unloading. Moreover, all the materials were considered to exhibit isotropic behaviour. For this reason, the materials can be completely defined by its Elastic Modulus (E) and Poisson's ratio (ν). Furthermore, the relationship between the components of stress and strain can be given by the Hooke's Law.

The present work was developed in two-dimensions, considering the plane strain or the plane stress assumptions. In this work we aim to analyse the von Mises stress and the equivalent strain obtained in skin. Accordingly, the von Mises stress for each interest point, \mathbf{x}_I , can be calculated using Eq.(1) and the equivalent strain for each interest point, \mathbf{x}_I , can also be obtained using Eq.(2). The fully description of all the concepts and formulation in this area is presented in [7].

$$\bar{\sigma}(\mathbf{x}_I) = \sqrt{\frac{1}{2}[(\sigma(\mathbf{x}_I)_1 - \sigma(\mathbf{x}_I)_2)^2 + (\sigma(\mathbf{x}_I)_2 - \sigma(\mathbf{x}_I)_3)^2 + (\sigma(\mathbf{x}_I)_3 - \sigma(\mathbf{x}_I)_1)^2]} \quad (1)$$

$$\bar{\varepsilon}(\mathbf{x}_I) = \sqrt{\frac{2}{3}[(\varepsilon(\mathbf{x}_I)_1 - \varepsilon_m)^2 + (\varepsilon(\mathbf{x}_I)_2 - \varepsilon_m)^2 + (\varepsilon(\mathbf{x}_I)_3 - \varepsilon_m)^2]} \quad (2)$$

2.3. Numerical model

In this work, we developed 2D models aimed to simulate the suturing process and to analyse the von Mises stress and the equivalent stain obtained during the process, using FEM and NNRPIM analysis. All the numerical simulations were performed using the software FEMAS. In Fig. 1 the geometry and boundary conditions used are presented. Concerning model A, several points in the boundary were selected and it was applied a force value in each one in order to mimic the stitches made with the needle during suturing in the area around the wound, as illustrated in Fig. 1. In the following models (B, C and D) more specific points were consecutively selected and a similar force was applied in each one, as illustrated in Fig. 1. In Table 1 the model dimensions and the material properties of each skin layer used to constructed the models are presented.

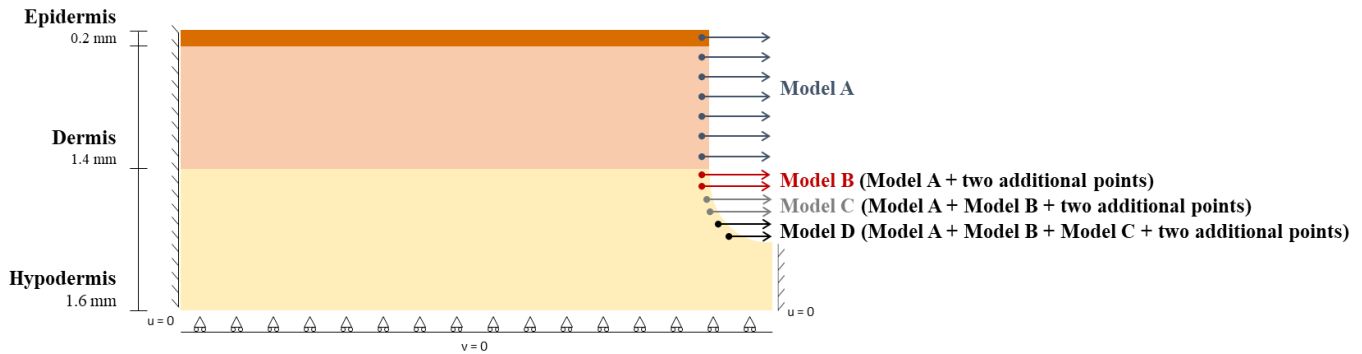


Fig. 1 - Model geometry and boundary conditions for model A, model B, model C and model D.

Table 1 - Model dimensions and material properties [10, 11].

Skin layer	Elastic Modulus (E) - MPa	Poisson's coefficient (ν)
Epidermis	102	0.48
Dermis	10.2	0.48
Hypodermis	0.0102	0.48

3. Results

In this section, we will only present the results obtained in the hypodermis. In epidermis and dermis the stress and strain fields achieved were very high and homogeneous related to the same layer. The results obtained for the von Mises stress for model A, in which it was applied a force in the boundary of epidermis and dermis in order to simulate the suturing process, are presented in Fig. 2. Analysing the von Mises stress isomaps (Fig. 2(a)) it is possible to observe that the highest stress levels (around 8×10^{-3} MPa) were obtained in the surrounding wound area and in the transition from the hypodermis to the dermis, in FEM and NNRPIM analysis. The measurement of this parameter in specific points around the wound (Fig. 2(b)) confirms this observation.

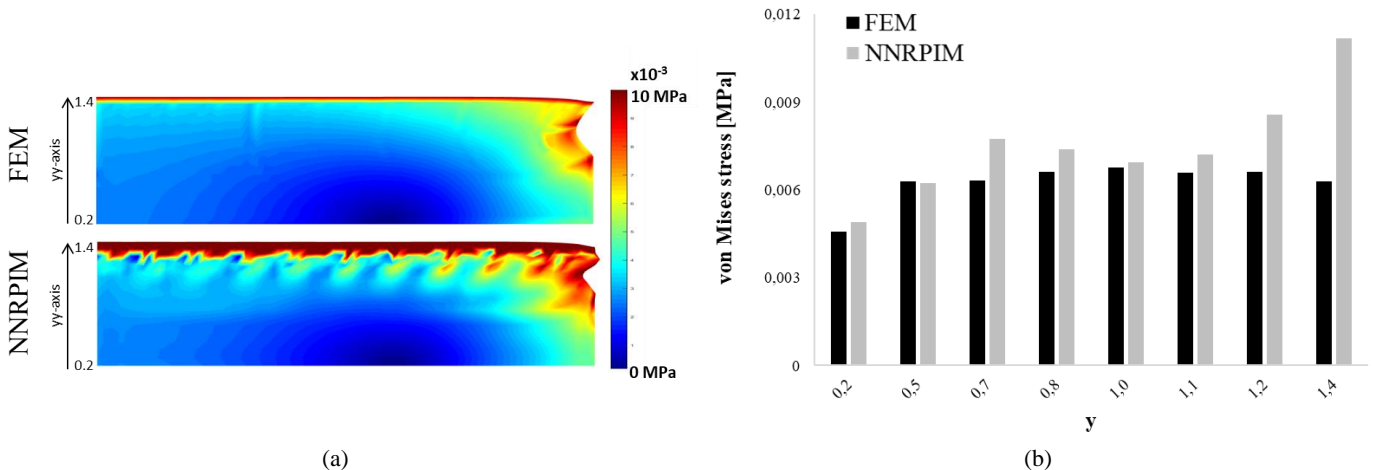


Fig. 2 - (a) von Mises stress isomaps obtained with FEM and NNRPIM for model A; (b) von Mises stress measured in specific points in the area around the wound, in the two advanced discretization techniques.

The results obtained for the equivalent strain for the same model are presented in Fig. 3. Analysing the equivalent strain isomaps (Fig. 3(a)) and the graph (Fig. 3(b)) it is possible to observe that the highest strain levels, around 0.6, were obtained in the area around the wound, in FEM and NNRPIM analysis.

The results obtained for the von Mises stress for model B, in which it was applied a force in the boundary of epidermis, dermis and hypodermis in order to simulate the suturing process, are presented in Fig. 4. Analysing the von Mises stress isomaps (Fig. 4(a)) and the graph (Fig. 4(b)) it is possible to observe that the highest stress levels (around 8×10^{-3} MPa)

were obtained in the surrounding wound area, in FEM and NNRPIM analysis. It was also obtained high von Mises stress levels in the transition from the hypodermis to the dermis (Fig. 4(a)).

The results obtained for the equivalent strain for the same model are presented in Fig. 5. Analysing the equivalent strain isomaps (Fig. 5(a)) and the graph (Fig. 5(b)) it is possible to observe that the highest strain levels, around 0.8, were obtained in the area around the wound, in both advanced discretization techniques used.

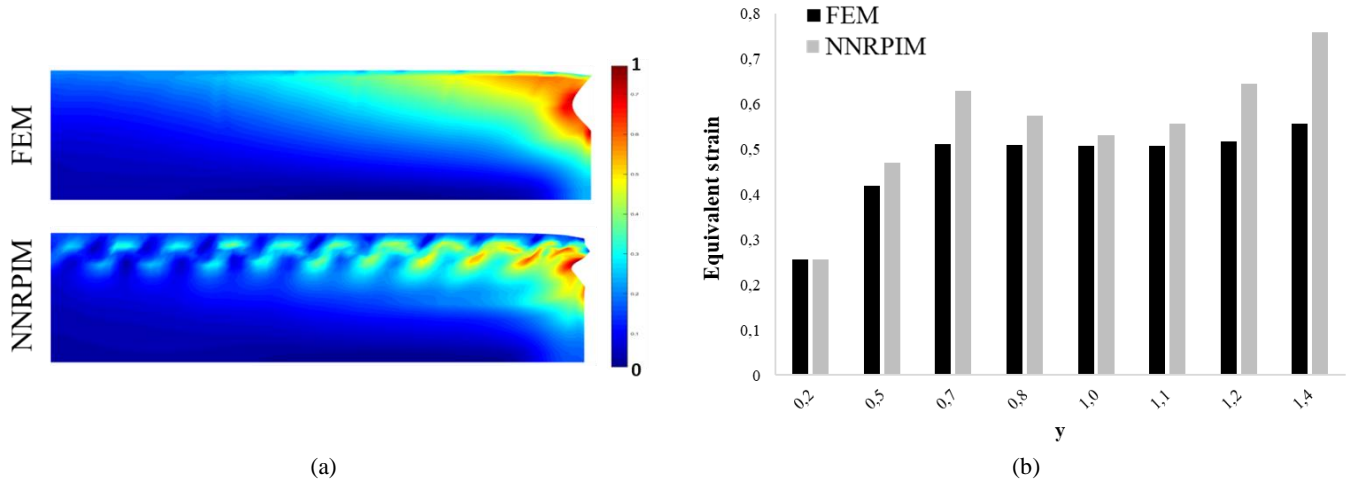


Fig. 3 - (a) Equivalent strain isomaps obtained with FEM and NNRPIM for model A; (b) Equivalent strain measured in specific points in the area around the wound, in the two advanced discretization techniques.

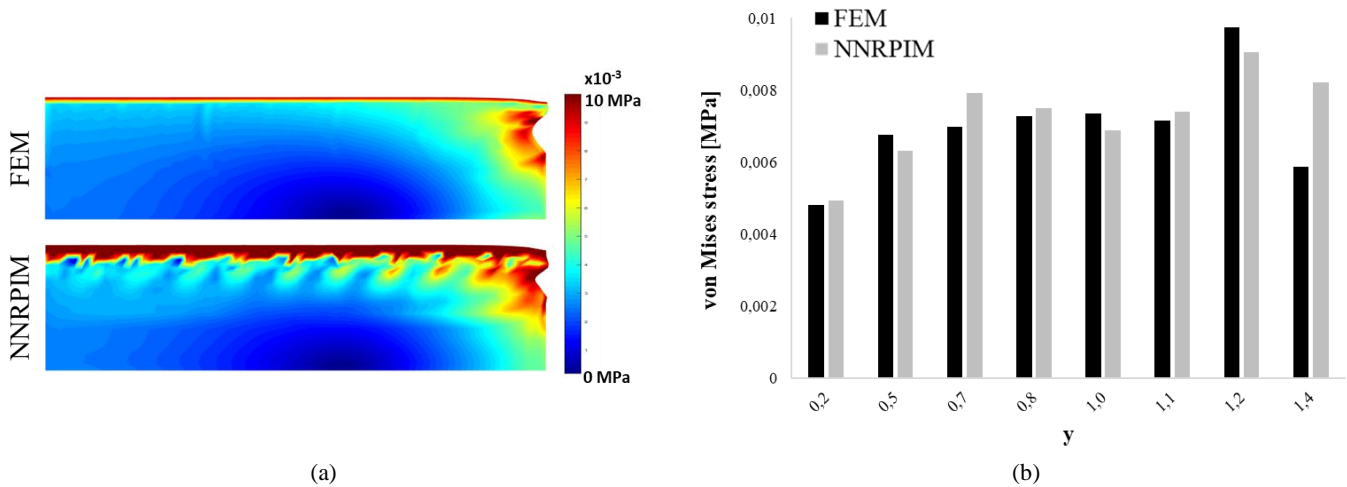


Fig. 4 – (a) von Mises stress isomaps obtained with FEM and NNRPIM for model B; (b) von Mises stress measured in specific points in the area around the wound, in the two advanced discretization techniques.

The results obtained for the von Mises stress for model C, in which it was consecutively applied a force in more points in the boundary of hypodermis in order to simulate the suturing process, are presented in Fig. 6. Analysing the von Mises stress isomaps (Fig. 6(a)) and the graph (Fig. 6(b)) it is possible to observe that the highest stress levels (around 9×10^{-3} MPa) were obtained in the surrounding wound area, in FEM and NNRPIM analysis. Once again, it was also obtained high von Mises stress levels in the transition from the hypodermis to the dermis (Fig 6(a)).

The results obtained for the equivalent strain for the same model are presented in Fig. 7. Analysing the equivalent strain isomaps (Fig. 7(a)) and the graph (Fig. 7(b)) it is possible to confirm that the highest strain levels, around 0.8, were obtained in the area around the wound, in FEM and NNRPIM analysis.

The results obtained for the von Mises stress for model D, in which it was consecutively applied a force in more points filling in the entire wound, are presented in Fig. 8. Analysing the von Mises stress isomaps (Fig. 8(a)) and the graph (Fig. 8(b)) it is possible to observe that the highest stress levels (around 8×10^{-3} MPa) were obtained in the surrounding wound area, in FEM and NNRPIM analysis. Moreover, it was also obtained high von Mises stress levels in the transition from

the hypodermis to the dermis, in the both techniques used. Analysing the advanced discretization techniques solution isomaps (Fig. 8(a)) it is also possible to observe that the wound is practically closed.

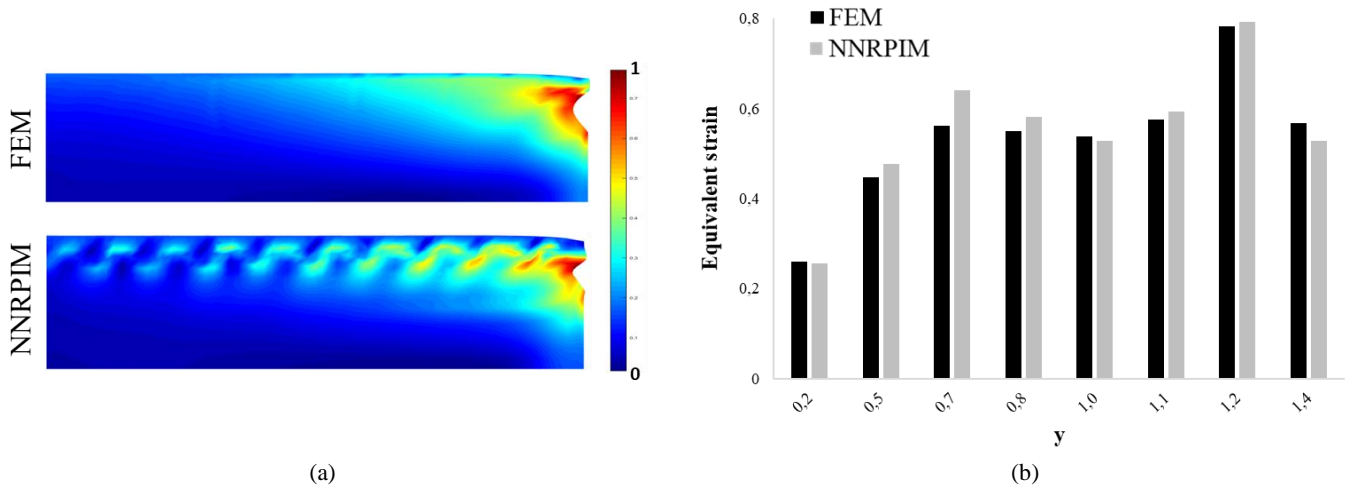


Fig. 5 - (a) Equivalent strain isomaps obtained with FEM and NNRPIM for model B; (b) Equivalent strain measured in specific points in the area around the wound, in the two advanced discretization techniques.

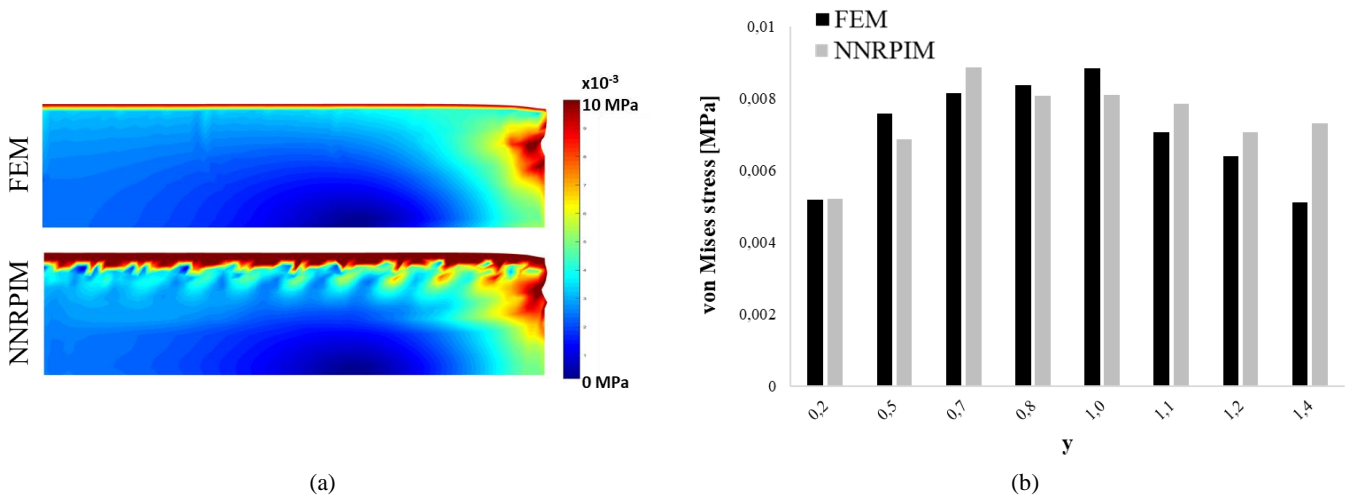


Fig. 6 - (a) von Mises stress isomaps obtained with FEM and NNRPIM for model C; (b) von Mises stress measured in specific points in the area around the wound, in the two advanced discretization techniques.

The results obtained for the equivalent strain for the same model are presented in Fig. 9. Analysing the equivalent strain isomaps (Fig. 9(a)) and the graph (Fig. 9(b)) it is possible to observe that the highest strain levels, around 0.8, were obtained in the area around the wound, in both advanced discretization techniques used.

4. Discussion and Conclusions

Computational models are very useful to simulate mechanical and biochemical problems in order to improve humans' health. FEM is a powerful numerical method that allows to deal with irregular boundaries, general loads, nonlinear problems, different materials and boundary conditions, it permits to create meshes with variable element size and it is easy to modify and dynamic [12]. Comparatively to FEM, meshless methods have the re-meshing efficiency, which allows to deal with large distortions of soft materials, such as the skin [7]. Moreover, these methodologies are less expensive and time consuming when compared with the experimental ones.

In this work, FEM and NNRPIM analysis were used to study the stress and strain fields obtained in the skin during the suturing process. In our models, the highest levels of stress (around 8×10^{-3} MPa) and strain (around 0.8 and 0.6) were obtained in the area around the wound. Moreover, high levels of stress were also obtained in the transition between the hypodermis and the dermis. In models C and D, in the end of the simulations, the wound is practically closed. We are

aware that the mechanical properties of the healthy and wounded skin tissue are different. However, the aim of this work was to analyse the stress and strain fields obtained in all the skin layer when the suture occurs. Therefore, we only used the mechanical properties related to healthy skin.

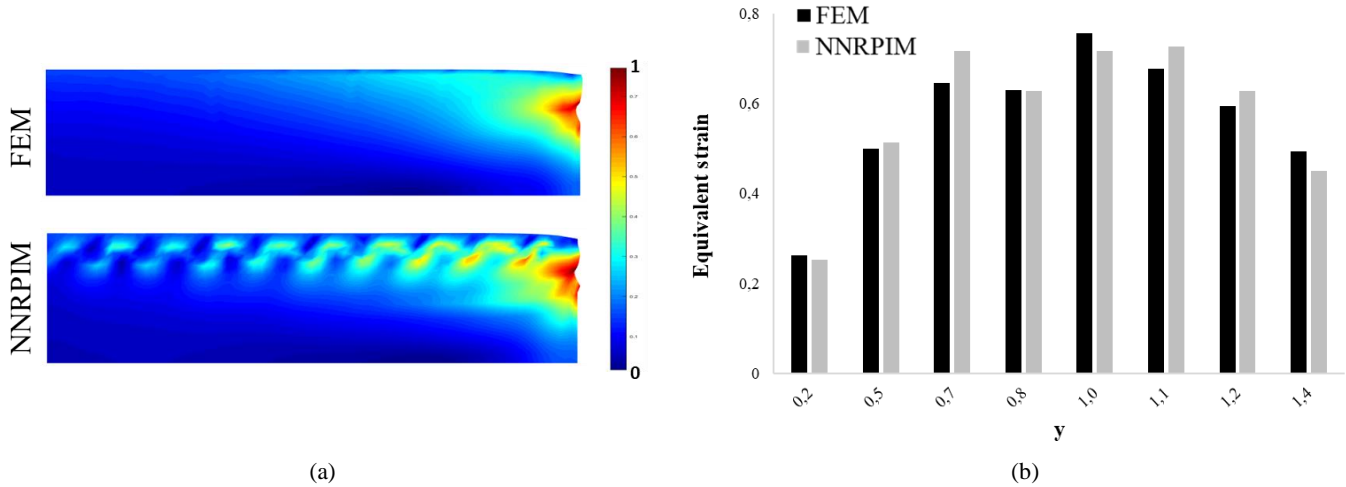


Fig. 7 - (a) Equivalent strain isomaps obtained with FEM and NNRPIM for model C; (b) Equivalent strain measured in specific points in the area around the wound, in the two advanced discretization techniques.

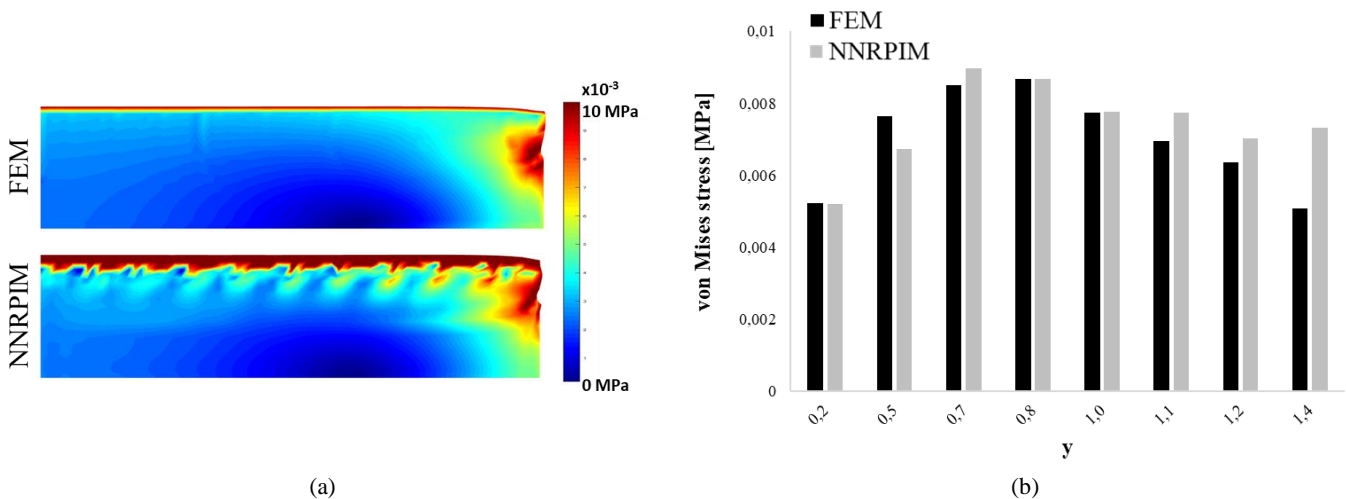


Fig. 8 - (a) von Mises stress isomaps obtained with FEM and NNRPIM for model D; (b) von Mises stress measured in specific points in the area around the wound, in the two advanced discretization techniques.

Human skin exhibits nonlinear stress-strain, anisotropic and viscoelastic characteristics [13]. Nevertheless, in order to decrease the model's complexity, most of the studies assume skin as an isotropic and linear elastic material [14]. Accordingly, in this study the skin was modelled as an isotropic and linear elastic material.

Although this is a preliminary study to evaluate the performance of these numerical methods in the analysis of stress profile in human skin it was possible to conclude that FEM and NNRPIM are valid numerical tools. The numerical methods used in the simulations demonstrated equivalent results. Moreover, the materials used in the simulations were well characterized in terms of elasticity. In the future, it is intended that this kind of models could assist surgeons during surgery planning in order to recognize the regions of stress and strain concentration to improve the healing of sutured wounds. Despite the simplifications, the wound closure model presented in this paper is a useful tool for evaluating the merits of different excision shapes and improving the healing of sutured wounds.

Acknowledgements and Funding

The authors truly acknowledge the funding provided by Ministério da Ciência, Tecnologia e Ensino Superior - Fundação para a Ciência e a Tecnologia (Portugal), under Grant SFRH/BD/133894/2017. Additionally, the authors acknowledge the funding provided by LAETA, under project UIDB/50022/2020.

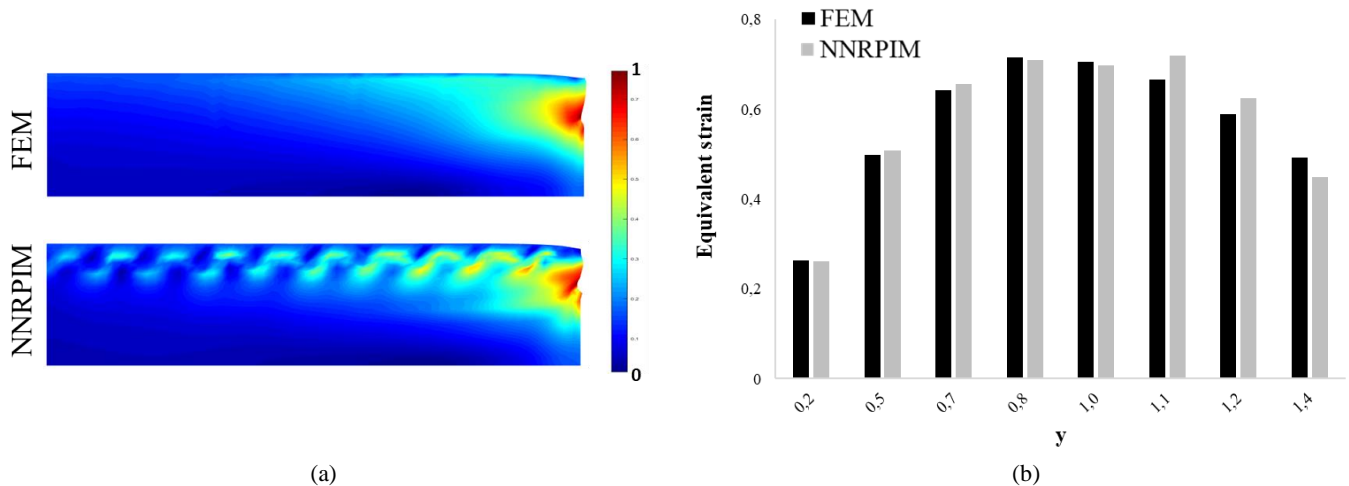


Fig. 9 - (a) Equivalent strain isomaps obtained with FEM and NNRPIM for model D; (b) Equivalent strain measured in specific points in the area around the wound, in the two advanced discretization techniques.

References

- [1] Reihnsner R, Balogh B, Menzel EJ. Two-dimensional elastic properties of human skin in terms of an incremental model at the in vivo configuration. *Med Eng Phys.* 1995;17(4):304-13.
- [2] Flynn C. Finite element models of wound closure. *J Tissue Viability.* 2010;19(4):137-49.
- [3] Wang P, Becker AA, Jones IA, Glover AT, Benford SD, Greenhalgh CM, et al. Virtual reality simulation of surgery with haptic feedback based on the boundary element method. *Computers & Structures.* 2007;85(7):331-9.
- [4] Yang C, Tang D, Haber I, Geva T, del Nido PJ. In vivo MRI-based 3D FSI RV/LV models for human right ventricle and patch design for potential computer-aided surgery optimization. *Computers & Structures.* 2007;85(11):988-97.
- [5] Cavicchi A, Gambarotta L, Massabò R. Computational modeling of reconstructive surgery: The effects of the natural tension on skin wrinkling. *Finite Elem Anal Des.* 2009;45(8):519-29.
- [6] Fish J, Belytschko T. *A First Course in Finite Elements*: John Wiley & Sons; 2007.
- [7] Belinha J. *Meshless Methods in Biomechanics - Bone Tissue Remodelling Analysis*: Springer International Publishing; 2014.
- [8] Belinha J, Dinis LMJS, Jorge RMN. The analysis of the bone remodelling around femoral stems. *Math Comput Simul.* 2016;121(C):64-94.
- [9] Dinis LMJS, Natal Jorge RM, Belinha J. Analysis of 3D solids using the natural neighbour radial point interpolation method. *Comput Methods Appl Mech Eng.* 2007;196(13):2009-28.
- [10] Areias P, Natal Jorge R, Barbosa J, Fernandes A, Mascarenhas T, Oliveira M, et al. *Experimental and Finite Element Analysis of Human Skin Elasticity* 2003.
- [11] Li C, Guan G, Reif R, Huang Z, Wang R. Determining elastic properties of skin by measuring surface waves from an impulse mechanical stimulus using phase-sensitive optical coherence tomography. *Journal of the Royal Society, Interface / the Royal Society.* 2011;9:831-41.
- [12] Belinha J, Dinis LMJS, Natal Jorge RM. The analysis of the bone remodelling around femoral stems: A meshless approach. *Math Comput Simul.* 2016;121:64-94.
- [13] Silver FH, Freeman JW, DeVore D. Viscoelastic properties of human skin and processed dermis. *Skin Res Technol.* 2001;7(1):18-23.
- [14] Zahouani H, Pailler-Mattei C, Sohm B, Vargiolu R, Cenizo V, Debret R. Characterization of the mechanical properties of a dermal equivalent compared with human skin in vivo by indentation and static friction tests. *Skin Res Technol.* 2009;15(1):68-76.